


Novel Turbo Receiver for MU-MIMO SC-FDMA System

Hung-Sheng Wang, Fang-Biau Ueng  and Yu-Kuan Chang

Single carrier-frequency-division multiple access (SC-FDMA) has been adopted as the uplink transmission standard in fourth-generation cellular networks to facilitate power efficiency transmission in mobile stations. Because multiuser multiple-input multiple-output (MU-MIMO) is a promising technology employed to fully exploit the channel capacity in mobile radio networks, this study investigates the uplink transmission of MU-MIMO SC-FDMA systems with orthogonal space-frequency block codes (SFBCs). It is preferable to minimize the length of the cyclic prefix (CP). In this study, the chained turbo equalization technique with chained turbo estimation is employed in the designed receiver. Chained turbo estimation employs a short training sequence to improve the spectrum efficiency without compromising the estimation accuracy. In this paper, we propose a novel and spectrally efficient iterative joint-channel estimation, multiuser detection, and turbo equalization for an MU-MIMO SC-FDMA system without CP-insertion and with short TR. Some simulation examples are presented for the uplink scenario to demonstrate the effectiveness of the proposed scheme.

Keywords: Chained turbo estimation, Chained turbo equalization, MU-MIMO, SC-FDMA.

1. Introduction

The uplink of long-term evolution (LTE) employs single-carrier frequency-division multiple access (SC-FDMA) [1], and the downlink uses orthogonal frequency-division multiple access (OFDMA) [2]. Compared to OFDM, SC-FDMA has a lower peak-to-average power ratio (PAPR) [3], [4]. Multiuser multiple-input multiple-output (MU-MIMO) [5] can leverage multiple users as spatially distributed transmission resources at the expense of somewhat more expensive signal processing. Thus, MU-MIMO is also known as spatial-division multiple access (SDMA). MU-MIMO algorithms are developed to enhance MIMO systems when there are multiple users within the same frequency band. Iterative multiuser detection, which is also known as turbo multiuser detection [6], and which is based on the turbo principle [7], has attracted much attention in recent studies. The channel decoder and multiuser detector iterate soft information to cancel multiple-access interference.

In general, SC-FDMA systems employ cyclic prefixes (CPs) to resist inter-block interference (IBI) due to the multipath fading propagation. With CP, the channel matrix becomes a circular structure, and can reduce the complexity of signal detection [8], [9]. Fifth-generation (5G) communications systems need to handle a wide range of applications. The low latency required for Tactile Internet and vehicle-to-vehicle applications results in the need for short bursts of data, meaning that OFDM signals with one CP per symbol would present a prohibitively low spectral efficiency. The low spectrum efficiency due to the CP insertion is also a problem for wireless regional area network applications, where the typical channel impulse response has a duration of several tens of microseconds. In this study, we eliminate the CP at the MU-MIMO SC-FDMA transmitter and introduce the chained turbo equalization version 2 (CHATUE2) with chained turbo estimation (CHATES) [10] at the receiver. CHATUE [11] employs a matrix [12] to retrieve the channel matrix.

Manuscript received Sept. 26, 2017; revised Dec. 26, 2017; accepted Jan. 25, 2018.

Hung-Sheng Wang (49830105@gm.nfu.edu.tw), Fang-Biau Ueng (corresponding author, fbueing@nchu.edu.tw), and Yu-Kuan Chang (changyukuan@hotmail.com) are with the Department of Electrical Engineering, National Chung-Hsing University, Taichung, Taiwan.

This is an Open Access article distributed under the term of Korea Open Government License (KOGI) Type 4: Source Indication + Commercial Use Prohibition + Change Prohibition (<http://www.kogil.or.kr/info/licenseTypeEn.do>).

CHATUE2 renews the algorithm of CHATUE to obtain a better signal-to-noise ratio (SNR) at the equalizer output. This method [13] uses IBI cancellation for the training sequence (TR) and single-burst channel estimation. Therefore, CHATUE2 with CHATES can improve the system power and spectrum efficiency. In this paper, we propose a novel spectrally efficient iterative joint channel estimation, multiuser detection (MUD) and turbo equalization for MU-MIMO SC-FDMA systems without CP-insertion and with a short TR. We compare the performance of the proposed scheme with that of turbo equalization with an adequate turbo equalization CP (TEQ-CP) [14]. Simulation results show that the proposed scheme outperforms the TEQ-CP. Several techniques have been investigated for block transmission without CP-insertion [15]–[20]. Reference [12] proposed block transmission without CP-insertion by assuming that the previous component was perfectly cancelled, where the Bayesian linear unbiased estimation (BLUE) approach was utilized to predict the interference components from the future block. Reference [15] proposed a novel frequency-domain TEQ technique for SC-FDMA systems without CP-insertion by making several relevant modifications to the CHATUE algorithm [11] because SC-FDMA systems have subcarrier mapping. Although they introduced channel estimation, MUD, and equalization, the transmitter also needs to insert a CP [20]. In this study, we employ CHATUE2 and CHATES, and we used space-frequency block code (SFBC)-based MUD to develop a novel spectrally efficient iterative joint channel estimation, MUD, and TEQ for MU-MIMO SC-FDMA systems without CP-insertion and with short TR.

Notation: Vectors and matrices are denoted by boldface letters; the superscripts $(\cdot)^*$, $(\cdot)^T$, $(\cdot)^H$, $(\cdot)^{-1}$, and \otimes denote the complex conjugate, transpose, conjugate transpose, inverse, and convolution, respectively; $\text{diag}\{\cdot\}$ denotes the diagonal matrix; \mathbf{I}_p is the $P \times P$ identity matrix; $E\{\cdot\}$ denotes the statistical expectation; $\text{tr}(\cdot)$ denotes the trace of its argument; and $\Re\{\cdot\}$ represents the real parts of the element in the brackets.

II. System Model

In this section, we describe the uplink MU-MIMO SC-FDMA communication system. For the u -th user, we assume that each modulated symbol $x^{(u)}(m)$ is a binary phase shift keying (BPSK)/quadrature PSK (QPSK) signal within the m -th symbol time. After applying an M -point discrete Fourier transform (DFT), the signal can be written as

$$\mathbf{X}^{(u)} = \mathbf{F}_M x^{(u)}, \quad (1)$$

where \mathbf{F}_M is the M -point DFT matrix. The element of the matrix can be written as

$$[\mathbf{F}_M]_{a,b} = \frac{1}{\sqrt{M}} \exp(-j2\pi ab/M), \quad a, b \in \{0, \dots, M-1\}. \quad (2)$$

We employed the SFBC. For simplicity, to explain the operation of SFBC, we assume two transmitting antennas and two receiving antennas. First, the signal of (1) should be separated into two components, that is, an even frequency signal and an odd frequency signal. The even frequency signal of the first antenna transmits $\mathbf{X}_{2i}^{(u)}$, the odd frequency signal of the first antenna transmits $-\mathbf{X}_{2i+1}^{(u)*}$, the even frequency signal of the second antenna transmits $\mathbf{X}_{2i+1}^{(u)}$, and the odd frequency signal of the second antenna transmits $\mathbf{X}_{2i}^{(u)*}$. After SFBC mapping, we use interleaved subcarrier mapping to fill up zeros in order to satisfy an N -point inverse discrete Fourier transform (IDFT) matrix. We also insert a block-type TR to obtain the initial channel estimation of the channel for the equalizer and the MUD. The signal becomes $\bar{\mathbf{S}}_{n_t}^{(u)}$, and CP-insertion is not needed. We define L_p as the length of the TR. Using the fading channel, we collect all N_t transmitting antennas into an $(N + L_{cp} + L_p) \times N_t$ matrix. We define

$$\bar{\mathbf{S}}_{n_t}^{(u)} = \left[\bar{S}_{n_t}^{(u)}(0) \quad \bar{S}_{n_t}^{(u)}(1) \quad \dots \quad \bar{S}_{n_t}^{(u)}(N + L_{cp} + L_p - 1) \right]^T, \quad (3)$$

which means that the combined signal becomes $\bar{\mathbf{S}}^{(u)} = [\bar{\mathbf{S}}_1^{(u)}, \bar{\mathbf{S}}_2^{(u)}, \dots, \bar{\mathbf{S}}_{N_t}^{(u)}]$. The signal at the n_r -th receiver antenna is denoted as r_{n_r} , that is

$$\mathbf{r}_{n_r} = \sum_{u=1}^U \tilde{\mathbf{h}}_{n_r, n_t}^{(u)} \otimes \bar{\mathbf{S}}^{(u)} + \mathbf{q}_{n_r}, \quad (4)$$

where $\tilde{\mathbf{h}}_{n_r, n_t}^{(u)}$ is an $(N_r W) \times N_t$ channel matrix that can be described as follows

$$\tilde{\mathbf{h}}_{n_r, n_t}^{(u)} = \begin{pmatrix} \mathbf{h}_{1,1}^{(u)} & \mathbf{h}_{1,2}^{(u)} & \dots & \mathbf{h}_{1,N_t}^{(u)} \\ \mathbf{h}_{2,1}^{(u)} & \mathbf{h}_{2,2}^{(u)} & \dots & \mathbf{h}_{2,N_t}^{(u)} \\ \vdots & \vdots & \ddots & \vdots \\ \mathbf{h}_{N_r,1}^{(u)} & \mathbf{h}_{N_r,2}^{(u)} & \dots & \mathbf{h}_{N_r,N_t}^{(u)} \end{pmatrix}. \quad (5)$$

The element vector of the channel matrix is a W -tap channel impulse response (CIR) vector, which is given as follows:

$$\mathbf{h}_{a,b}^{(u)} = [h_{a,b}(0) \quad h_{a,b}(1) \quad \dots \quad h_{a,b}(W-1)]^T, \quad (6)$$

where (4) indicates that the transmitted signals $\bar{\mathbf{S}}^{(u)}$ are convolved with channel $\mathbf{h}_{n_r, n_t}^{(u)}$, and \mathbf{q}_{n_r} is complex additive

white Gaussian noise. After N -point DFT and removing training symbols, the signal becomes

$$\bar{\mathbf{Y}}_{n_r} = \mathbf{F}_N \left(\sum_{u=1}^U \tilde{\mathbf{h}}_{n_r, n_t}^{(u)} \otimes \bar{\mathbf{S}}^{(u)} + \mathbf{q}_{n_r} \right) = \sum_{u=1}^U \tilde{\mathbf{H}}_{n_r, n_t}^{(u)} \mathbf{S}_{n_t}^{(u)} + \Lambda_{n_r} \quad (7)$$

where $\tilde{\mathbf{H}}_{n_r, n_t}^{(u)} = \mathbf{F}_N \tilde{\mathbf{h}}_{n_r, n_t}^{(u)}$, $\mathbf{S}_{n_t}^{(u)} = \mathbf{F}_N \bar{\mathbf{S}}^{(u)}$, $\Lambda_{n_r} = \mathbf{F}_N \mathbf{q}_{n_r}$, and \mathbf{F}_N is an N -point DFT matrix. A TR is used to provide initial channel estimation at the first iteration for CHATES. As shown in Fig. 1, the estimation algorithm executes IBI cancellation with the TR, and it then uses the asymptotic maximum-likelihood (AML) estimation algorithm to obtain the initial channel estimation for MUD and CHATUE. After DFT, subcarrier de-mapping as well as MUD, the signals are then sent to the CHATUE. First, the algorithm is executed to retrieve the channel matrix for the received signals. Secondly, the algorithm executes soft cancellation for the retrieved signal. Finally, we send the soft cancellation version of the retrieved signal to the frequency domain/single-carrier minimum mean squared error (FD/SC-MMSE) equalizer [10]. The equalizer outputs the extrinsic log-likelihood ratio (LLR) of the transmitted symbol for the next iteration. The LLR is then fed back from

the decoder to the equalizer, after which it computes the soft symbol.

III. MUD with Chained Turbo Estimation

We used TEQ to iteratively estimate the transmitted symbol. CHATES is employed to estimate the channel information. First, we used the TR to perform initial channel estimation. Next, we performed the MUD and equalization. The signals pass through a decoder and LLR computation is performed. The whole process runs iteratively to obtain an enhanced performance.

A. MUD Using SFBC Channel Property

After subcarrier demapping, MUD is then performed. Consider the case of two transmitting antennas, two receiver antennas, and two users in the same frequency band. The received signal can be written as follows:

$$\begin{bmatrix} Y_{1,2i} \\ Y_{1,2i+1} \end{bmatrix} = \begin{bmatrix} \hat{H}_{1,1} & \hat{H}_{1,2} \\ \hat{H}_{1,2}^* & -\hat{H}_{1,1}^* \end{bmatrix} \begin{bmatrix} X_{2i}^{(1)} \\ X_{2i+1}^{(1)} \end{bmatrix} + \begin{bmatrix} \hat{H}_{1,3} & \hat{H}_{1,4} \\ \hat{H}_{1,4}^* & -\hat{H}_{1,3}^* \end{bmatrix} \begin{bmatrix} X_{2i}^{(2)} \\ X_{2i+1}^{(2)} \end{bmatrix} + \begin{bmatrix} N_{1,2i} \\ N_{1,2i+1} \end{bmatrix}, \quad (8)$$

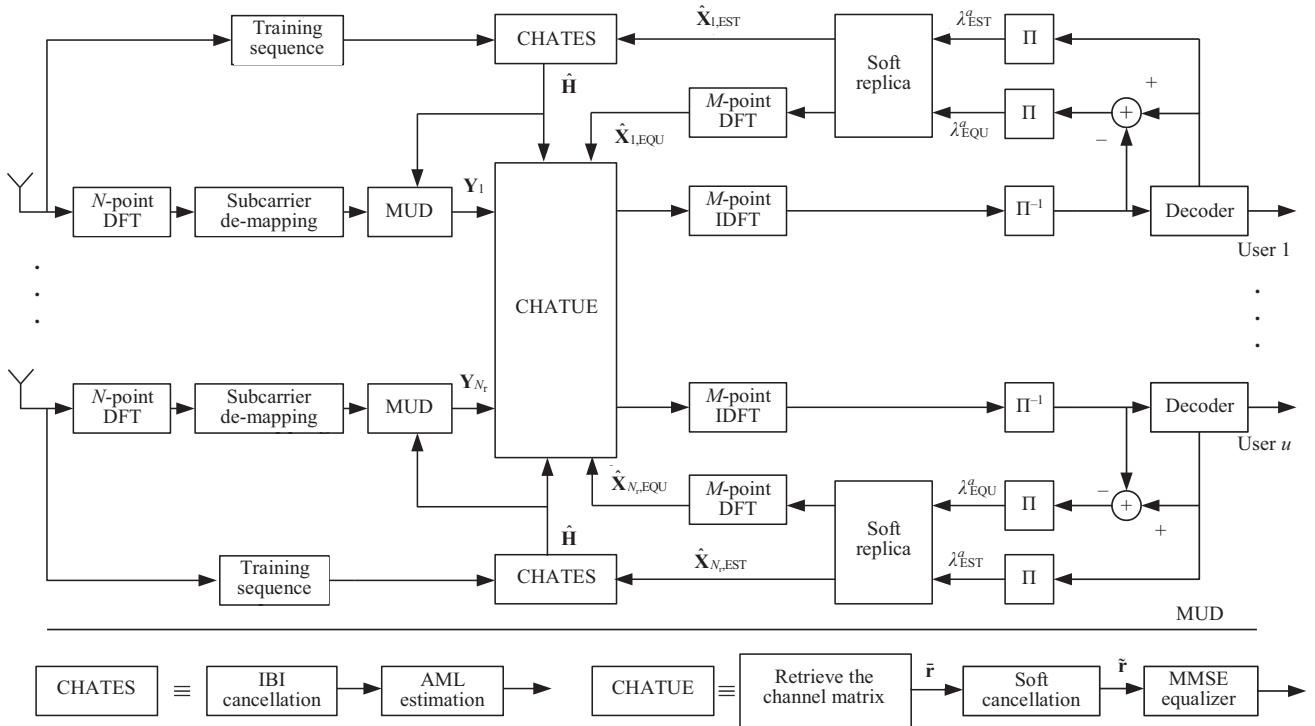


Fig. 1. Proposed turbo receiver for MU-MIMO SC-FDMA system.

$$\begin{bmatrix} Y_{2,2i} \\ Y_{2,2i+1} \end{bmatrix} = \begin{bmatrix} \hat{H}_{2,1} & \hat{H}_{2,2} \\ \hat{H}_{2,2}^* & -\hat{H}_{2,1}^* \end{bmatrix} \begin{bmatrix} X_{2i}^{(1)} \\ X_{2i+1}^{(1)} \end{bmatrix} + \begin{bmatrix} \hat{H}_{2,3} & \hat{H}_{2,4} \\ \hat{H}_{2,4}^* & -\hat{H}_{2,3}^* \end{bmatrix} \begin{bmatrix} X_{2i}^{(2)} \\ X_{2i+1}^{(2)} \end{bmatrix} + \begin{bmatrix} N_{2,2i} \\ N_{2,2i+1} \end{bmatrix}, \quad (9)$$

where the element $\hat{H}_{i,j}$ denotes the channel gain between the i -th receiving antenna and the j -th transmitting antenna. For any orthogonal SFBC, because of the property of SFBC mapping, the channel matrices are orthogonal matrices. In order to eliminate the effect of the second user, we multiply the received signal at the receiver antenna with the transposition of the channel matrix of the second user. Therefore, the detected signal of user 1 can be described as (10).

To eliminate the effect of the first user, we multiply the received signal at the receiver antenna by the transposition of the channel matrix of the first user. Therefore, the detected signal of user 2 can be described as (11).

For the general case of SFBC with U users in the same frequency band, each user employs N_t transmitting antennas, K frequency transmit diversity, and N_r receiver

antennas in the base station. To eliminate the signal from the user $u = 1$, we pre-multiply \mathbf{Y}_1 by $\mathbf{H}_1^{(1)H}$ and divide it by $\sum_{n=1}^{N_t} (\mathbf{H}_{n,1}^{(1)})^{2H}$. Next, we can subtract $\mathbf{X}^{(1)}$ from \mathbf{Y}_{N_r} , where $2 \leq N_r \leq N_R$ in (8), by multiplying \mathbf{Y}_{N_r} by $\mathbf{H}_{N_r}^{(1)H}$ and dividing by $\sum_{n=1}^{N_t} (\mathbf{H}_{n,N_r}^{(1)})^{2H}$. That is, we have the following equations for $2 \leq N_r \leq N_R$:

$$\begin{aligned} & \frac{\mathbf{H}_m^{(1)H} \mathbf{V}_m}{\sum_{n=1}^{N_t} (\mathbf{H}_{n,m}^{(1)})^2} - \frac{\mathbf{H}_1^{(1)H} \mathbf{V}_1^T}{\sum_{n=1}^{N_t} (\mathbf{H}_{n,1}^{(1)})^2} \\ & = \sum_{n=1}^{N_t} \left\{ \frac{\mathbf{H}_m^{(1)H} \mathbf{V}_m}{\sum_{n=1}^{N_t} (\mathbf{H}_{n,m}^{(1)})^2} - \frac{\mathbf{H}_1^{(1)H} \mathbf{V}_1^T}{\sum_{n=1}^{N_t} (\mathbf{H}_{n,1}^{(1)})^2} \right\} \mathbf{X}_m + \boldsymbol{\eta}_m \end{aligned} \quad (12)$$

where $\boldsymbol{\eta}_m$ is denoted as

$$\boldsymbol{\eta}_m = \frac{\boldsymbol{\eta}_m}{\sum_{n=1}^{N_t} (\mathbf{H}_{n,m}^{(1)})^2} - \frac{\boldsymbol{\eta}_1}{\sum_{n=1}^{N_t} (\mathbf{H}_{n,1}^{(1)})^2}. \quad (13)$$

Therefore, once we eliminate the signal of the first user, we can apply the same method [25] to the remaining $M - 1$ signals and eliminate the other users' signals.

$$\begin{aligned} \tilde{\mathbf{Y}}_1 &= \left\{ \frac{1}{(|\hat{H}_{1,3}|^2 + |\hat{H}_{1,4}|^2)} \begin{bmatrix} \hat{H}_{1,3} & \hat{H}_{1,4} \\ \hat{H}_{1,4}^* & -\hat{H}_{1,3}^* \end{bmatrix}^H \begin{bmatrix} \hat{H}_{1,1} & \hat{H}_{1,2} \\ \hat{H}_{1,2}^* & -\hat{H}_{1,1}^* \end{bmatrix} - \frac{1}{(|\hat{H}_{2,3}|^2 + |\hat{H}_{2,4}|^2)} \begin{bmatrix} \hat{H}_{2,3} & \hat{H}_{2,4} \\ \hat{H}_{2,4}^* & -\hat{H}_{2,3}^* \end{bmatrix}^H \begin{bmatrix} \hat{H}_{2,1} & \hat{H}_{2,2} \\ \hat{H}_{2,2}^* & -\hat{H}_{2,1}^* \end{bmatrix} \right\} \begin{bmatrix} X_{2i}^{(1)} \\ X_{2i+1}^{(1)} \end{bmatrix} \\ &+ \left\{ \frac{1}{(|\hat{H}_{1,3}|^2 + |\hat{H}_{1,4}|^2)} \begin{bmatrix} \hat{H}_{1,3} & \hat{H}_{1,4} \\ \hat{H}_{1,4}^* & -\hat{H}_{1,3}^* \end{bmatrix}^H \begin{bmatrix} N_{1,2i} \\ N_{1,2i+1} \end{bmatrix} - \frac{1}{(|\hat{H}_{2,3}|^2 + |\hat{H}_{2,4}|^2)} \begin{bmatrix} \hat{H}_{2,3} & \hat{H}_{2,4} \\ \hat{H}_{2,4}^* & -\hat{H}_{2,3}^* \end{bmatrix}^H \begin{bmatrix} N_{2,2i} \\ N_{2,2i+1} \end{bmatrix} \right\} \\ &= \tilde{\mathbf{H}}_1 \begin{bmatrix} X_{2i}^{(1)} \\ X_{2i+1}^{(1)} \end{bmatrix} + \begin{bmatrix} \tilde{N}_{2i} \\ \tilde{N}_{2i+1} \end{bmatrix}. \end{aligned} \quad (10)$$

$$\begin{aligned} \tilde{\mathbf{Y}}_2 &= \left\{ \frac{1}{(|\hat{H}_{1,1}|^2 + |\hat{H}_{1,2}|^2)} \begin{bmatrix} \hat{H}_{1,1} & \hat{H}_{1,2} \\ \hat{H}_{1,2}^* & -\hat{H}_{1,1}^* \end{bmatrix}^H \begin{bmatrix} \hat{H}_{1,3} & \hat{H}_{1,4} \\ \hat{H}_{1,4}^* & -\hat{H}_{1,3}^* \end{bmatrix} - \frac{1}{(|\hat{H}_{2,1}|^2 + |\hat{H}_{2,2}|^2)} \begin{bmatrix} \hat{H}_{2,1} & \hat{H}_{2,2} \\ \hat{H}_{2,2}^* & -\hat{H}_{2,1}^* \end{bmatrix}^H \begin{bmatrix} \hat{H}_{2,3} & \hat{H}_{2,4} \\ \hat{H}_{2,4}^* & -\hat{H}_{2,3}^* \end{bmatrix} \right\} \begin{bmatrix} X_{2i}^{(2)} \\ X_{2i+1}^{(2)} \end{bmatrix} \\ &+ \left\{ \frac{1}{(|\hat{H}_{1,1}|^2 + |\hat{H}_{1,2}|^2)} \begin{bmatrix} \hat{H}_{1,1} & \hat{H}_{1,2} \\ \hat{H}_{1,2}^* & -\hat{H}_{1,1}^* \end{bmatrix}^H \begin{bmatrix} N_{1,2i} \\ N_{1,2i+1} \end{bmatrix} - \frac{1}{(|\hat{H}_{2,1}|^2 + |\hat{H}_{2,2}|^2)} \begin{bmatrix} \hat{H}_{2,1} & \hat{H}_{2,2} \\ \hat{H}_{2,2}^* & -\hat{H}_{2,1}^* \end{bmatrix}^H \begin{bmatrix} N_{2,2i} \\ N_{2,2i+1} \end{bmatrix} \right\} \\ &= \tilde{\mathbf{H}}_2 \begin{bmatrix} X_{2i}^{(2)} \\ X_{2i+1}^{(2)} \end{bmatrix} + \begin{bmatrix} \tilde{W}_{2i} \\ \tilde{W}_{2i+1} \end{bmatrix}. \end{aligned} \quad (11)$$

B. Chained Turbo Equalization

After removing the TR and performing DFT, subcarrier de-mapping, and MUD, the j -th received signals can be described as follows:

$$Y_j(l) = \mathbf{H}_j(l)\mathbf{X}_j(l) + \mathbf{H}'_j(l)\mathbf{X}'_j(l) + \mathbf{H}'_j(l+1)\mathbf{X}'_j(l+1) + \mathbf{n}_j, \quad (14)$$

where $\mathbf{H}'_j(l)\mathbf{X}'_j(l)$, $\mathbf{H}_j(l)\mathbf{X}_j(l)$, and $\mathbf{H}'_j(l+1)\mathbf{X}'_j(l+1)$ are the past, present, and future blocks, respectively. The IBI component $\mathbf{H}'_j(l)\mathbf{X}'_j(l)$ and $\mathbf{H}'_j(l+1)\mathbf{X}'_j(l+1)$ are known by employing TR. \mathbf{n}_j is a complex AWGN vector. $\mathbf{H}'_j(l)$ is a Toeplitz matrix, and it is used to perform the convolution of the transmitted data symbols and the CIR in the current block. If the CP is appended at the transmitter side and eliminated at the receiver side, the equivalent channel matrix becomes circulant. However, CP transmission is not employed in this study, and the channel matrix becomes a Toeplitz structure. Because the structure increases the computation complexity at the equalizer, we utilized the method in [10] to retrieve the channel matrix. The retrieved signals of the j -th received signals are defined as

$$\bar{\mathbf{R}}_j(l) \triangleq \mathbf{J}_R(1 - \eta)Y_j(l) + \mathbf{G}_R(\eta)\hat{Y}_j(l). \quad (15)$$

Then, the matrices \mathbf{J}_R and \mathbf{G}_R are defined as follows:

$$\mathbf{J}_R(1 - \eta) = \begin{bmatrix} \mathbf{0}_{(N_d-L) \times L} & \mathbf{I}_{N_d} \\ (1 - \eta)\mathbf{I}_L & \mathbf{0}_{N_d} \end{bmatrix} \in N_d \times (N_d + L), \quad (16)$$

$$\mathbf{G}_R(\eta) = \begin{bmatrix} 0_{N_d} & \mathbf{0}_{(N_d-L) \times L} \\ \eta\mathbf{I}_L & \mathbf{0}_{N_d} \end{bmatrix} \in N_d \times (N_d + L). \quad (17)$$

The factor η is defined as the mean-squared error (MSE) between $\bar{Y}_j(k; l; \eta)$ and $\mathbf{V}_j(l) = \mathbf{H}_j(l)\mathbf{X}_j(l) + \mathbf{H}'_j(l)\mathbf{X}'_j(l) + \mathbf{H}'_j(l+1)\mathbf{X}'_j(l+1)$, and it can be obtained as follows.

$$\eta = \underset{\eta}{\operatorname{argmin}} E \left[\|\mathbf{V}_j(l) - \bar{\mathbf{Y}}_j(l; \eta)\|^2 \right] \quad (18)$$

where $\bar{Y}_j(l; \eta) = (1 - \eta)Y_j(l) + \eta\hat{Y}_j(l)$ and the differential of (18) can be written as follows:

$$\frac{d}{d\eta} \operatorname{argmin} E \left[\|\mathbf{V}_j(l) - \bar{\mathbf{Y}}_j(l; \eta)\|^2 \right] = 0. \quad (19)$$

Therefore, the solution of (19) is

$$\eta = \frac{\sigma_{j,n}^2}{E \left[\|\mathbf{Y}_j(l) - \hat{\mathbf{Y}}_j(l)\|^2 \right]}, \quad (20)$$

where $\sigma_{j,n}^2$ is the variance of the AWGN. After retrieving the channel matrix, we need to remove the IBI component. Because CP is not transmitted, the signals suffer from IBI.

First, we constructed the soft replica of the retrieved signal, which is defined as

$$\hat{\mathbf{R}}_j(l) \triangleq \mathbf{J}_R(1 - \eta)\hat{\mathbf{Y}}_j(l) + \mathbf{G}_R(\eta)\hat{\mathbf{Y}}_j(l), \quad (21)$$

$$\hat{\mathbf{Y}}_j(l) = \hat{\mathbf{H}}_j(l)\hat{\mathbf{X}}_j(l) + \hat{\mathbf{H}}'_j(l)\hat{\mathbf{X}}'_j(l) + \hat{\mathbf{H}}'_j(l+1)\hat{\mathbf{X}}'_j(l+1), \quad (22)$$

$$\hat{\mathbf{X}}_j(l) = [\hat{X}_j(0; l), \hat{X}_j(1; l), \dots, \hat{X}_j(N_d; l)]. \quad (23)$$

The k -th symbol is given by

$$\hat{X}_j(k; l) = E[X_j(k; l)] = \tanh\{L_{a,E_l}[X_j(k; l)]/2\}. \quad (24)$$

Secondly, we decrease take $\bar{R}_j(l)$ to minus $\tilde{R}_j(l)$ in order to remove the interferences from the past, current, and future blocks. The remaining error can be defined as

$$\tilde{R}_j(l) = \bar{R}_j(l) - \hat{R}_j(l). \quad (25)$$

Because we need to estimate the k -th symbol, we should return the k -th symbol as follows:

$$\tilde{X}_j(k; l) = \tilde{R}_j(l) + \hat{H}_j(k; l)\hat{X}_j(k; l). \quad (26)$$

Finally, we need to reduce the remaining interference. The FD/SC-MMSE filter weight $w_j(k; l)$ can be determined as

$$\mathbf{w}_j(k; l) = \arg \min_{w_j^H(k; l)} |\mathbf{w}_j(k; l)^H \tilde{\mathbf{X}}_j(k; l) - \hat{\mathbf{X}}_j(k; l)|^2. \quad (27)$$

According to [10], the output is given by

$$z_j(l) = [\mathbf{I}_{N_d} + \mathbf{Q}_j(l)\hat{\mathbf{X}}_j(l)]^{-1} \cdot \left\{ \mathbf{Q}_j(l)\hat{x}_j(l) + \mathbf{F}^H \hat{\mathbf{\Theta}}_j(l)^H \delta_j(l)^{-1} \mathbf{F} \tilde{R}_j(l) \right\} \quad (28)$$

where $\hat{\mathbf{X}}_j(l) = \operatorname{diag} \left[\|\hat{x}_j(l)\|^2 \right]$, \mathbf{F} is the DFT matrix, and $\hat{\mathbf{\Theta}}_j(l) = \mathbf{F} \mathbf{J} \hat{\mathbf{H}}_j(l) \mathbf{F}^H$ is a diagonal matrix. The \mathbf{J} matrix was proposed in [12]. $\delta_j(l)$ is defined as

$$\delta_j(l) = \mathbf{F} \mathbf{v}_j(l) \mathbf{F}^H \quad (29)$$

where

$$\mathbf{v}_j(l) = \mathbf{J} \hat{\mathbf{H}}_j(l) \mathbf{M}(l) (\mathbf{J} \hat{\mathbf{H}}_j(l))^H + \mathbf{J} \hat{\mathbf{H}}'_j(l) \mathbf{M}(l) (\mathbf{J} \hat{\mathbf{H}}'_j(l))^H + \mathbf{J} \hat{\mathbf{H}}'_j(l+1) \mathbf{M}(l+1) (\mathbf{J} \hat{\mathbf{H}}'_j(l+1))^H + \sigma_{j,n}^2 \mathbf{J} \mathbf{J}^H \quad (30)$$

with $\mathbf{M}(l) = E \left[\{\hat{X}_j(l) - X_j(l)\} \{\hat{X}_j(l) - X_j(l)\}^H \right]$ and $\mathbf{M}'(l) = \mathbf{M}'(l+1) = \mathbf{0}$ because $X'_j(l)$ and $X'_j(l+1)$ are known TRs. Therefore, (29) can be described as follows:

$$\delta_j(l) \approx \hat{\Theta}_j(l) \mathbf{T}_j(l) \hat{\Theta}_j(l)^H + \sigma_{j,n}^2 \frac{N_d + (1 - \eta)L}{N_d} \mathbf{I}_{N_d} \quad (31)$$

where

$$\mathbf{T}_j(l) \approx \mathbf{F} \mathbf{M}(l) \mathbf{F}^H. \quad (32)$$

$\mathbf{Q}_j(l)$ can be approximated as follows:

$$\mathbf{Q}_j(l) \approx \frac{1}{N_d} \text{tr} \left[\hat{\Theta}_j(l)^H \delta_j(l)^{-1} \hat{\Theta}_j(l) \right] \mathbf{I}_{N_d}. \quad (33)$$

Finally, we approximated the j -th equalization output $z_j(l)$ as an equivalent Gaussian channel output that has input $\hat{x}_j(l)$,

$$z_j(l) = \mu_{j,z}(l) \hat{x}_j(l) + n_{j,z}(l). \quad (34)$$

The means of the j -th equalizer are derived as follows:

$$\mu_{j,z}(l) = \frac{1}{N_d} \text{tr} \left\{ \left(\mathbf{I}_{N_d} + \mathbf{Q}_j(l) \hat{X}_j(l) \right)^{-1} \mathbf{Q}_j(l) \right\} E \left[\|\hat{x}_j(l)\|^2 \right]. \quad (35)$$

Therefore, we converted the equalizer output into its corresponding extrinsic LLR as follows.

$$\lambda_{j,z}^\theta(l) = \frac{4\Re[z_j(l)]}{1 - \mu_{j,z}(l)}, \quad (36)$$

where $\Re[z_j(l)]$ represents the real component of the complex vector equalizer output.

C. Chained Turbo Estimation

Because the interference affects the estimation accuracy, we should assume the length of TR to be double the length of the CIR. However, the scheme will lower the spectral efficiency. The CHATES algorithm takes the received TR to perform interference cancellation, so the length of the TR may be equal to the CIR length without sacrificing estimation accuracy. The j -th received TR can be written as follows.

$$\mathbf{y}_{j,t}(l) = \mathbf{H}_{j,t}(l) \mathbf{X}_{j,t}(l) + \mathbf{H}'_{j,t}(l-1) \mathbf{X}'_{j,t}(l-1) + \mathbf{H}'_{j,t}(l) \mathbf{X}'_{j,t}(l) + \mathbf{n}_{j,t}. \quad (37)$$

The interferences are caused by the past and current block data symbols. We define the cancellation of the j -th received TR as follows.

$$\tilde{y}_{j,t}^{[k]}(l) = y_{j,t}(l) - \left[\hat{\mathbf{H}}_{j,t}^{[k-1]}(l-1) \hat{x}_{j,t}^{[k-1]}(l-1) + \hat{\mathbf{H}}_{j,t}^{[k-1]}(l) \hat{x}_{j,t}^{[k-1]}(l) \right]. \quad (38)$$

The factor k is defined as the k -th iteration. When $k = 1$, $\hat{\mathbf{H}}_{j,t}^{[k-1]}(l-1) = \hat{\mathbf{H}}_{j,t}^{[k-1]}(l) = 0$, and $\hat{x}_{j,t}^{[k-1]}(l-1) =$

$\hat{x}_{j,t}^{[k-1]}(l) = 0$. At the first iteration, we did not have the information of the symbol and channel estimates. After interference cancellation, we used the single-burst channel estimation as follows:

$$\hat{\mathbf{h}}(l) = \tilde{\mathbf{R}}_{j,XX}^{[k]}(l)^{-1} \tilde{\mathbf{R}}_{j,XY}^{[k]}(l) \quad (39)$$

where

$$\tilde{\mathbf{R}}_{j,XX}^{[k]}(l) = \tilde{\mathbf{X}}_{j,t}^H(l) \tilde{X}_{j,t}(l) + \beta^{[k-1]}(l) \hat{\mathbf{X}}_{j,d}^{[k-1]}(l)^H \hat{X}_{j,d}^{[k-1]}(l) \quad (40)$$

and

$$\tilde{\mathbf{R}}_{j,XY}^{[k]}(l) = \tilde{\mathbf{X}}_{j,t}^H(l) \tilde{Y}_{j,t}(l) + \beta_j^{[k-1]}(l) \hat{\mathbf{X}}_{j,d}^{[k-1]}(l)^H \hat{Y}_{j,d}^{[k-1]}(l). \quad (41)$$

The variable $\tilde{\mathbf{X}}_{j,t}^H(l)$ is defined as a Toeplitz matrix of the TR. $\hat{\mathbf{X}}_{j,d}^{[k-1]}(l)$ is defined as a Toeplitz matrix of the estimation of the data symbols. Because the soft-valued symbols are not perfect estimates, we regard the error as a white Gaussian process. Therefore, the factor $\beta^{[k-1]}$ is defined as

$$\beta_j^{[k-1]} = \frac{\sigma_{j,n}^2}{\left\{ \sigma_{j,n}^2 + \Delta \sigma_{j,d}^{[k-1]}(l)^2 \right\}} \quad (42)$$

where

$$\Delta \sigma_{j,d}^{[k-1]}(l)^2 = 1 - E \left[\|\hat{X}_{j,d}^{[k-1]}(l)\|^2 \right]. \quad (43)$$

IV. Simulation Results

We investigated the proposed scheme by performing bit error rate (BER) simulations. We evaluated the performances for a 2×2 QPSK MU-MIMO SC-FDMA system. The soft output Viterbi algorithm is used for decoding. Here, we describe the results of computer simulations to verify the feasibility and effectiveness of the proposed technique. For a good comparison, we considered the spectral efficiency of the structure of the burst format. In this section, we verify the performance of the proposed MU-MIMO SC-FDMA receiver using the Monte Carlo simulation method. Reference [21] provides an implementation of the spatial channel model (SCM). We simulated our proposed system in a suburban environment with six path taps, and in an urban environment with 14 path taps. For these systems, we assumed two users in the same frequency band simultaneously. Each user has two antennas for the uplink transmission, and two antennas at the receiver side. The simulated MU-MIMO SC-FDMA system has a fast

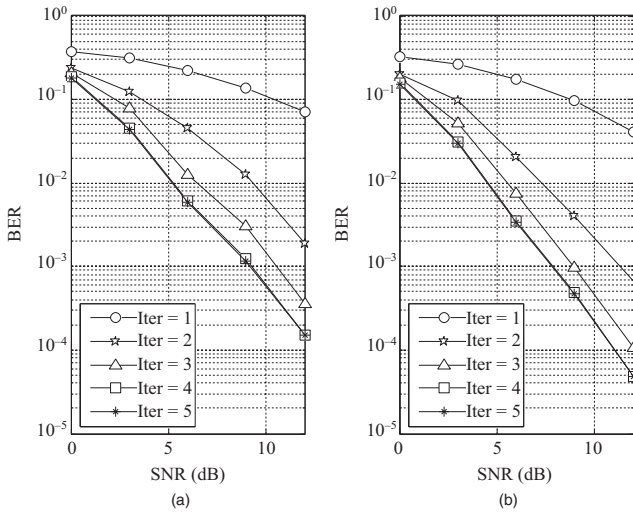


Fig. 2. Comparison of BER performance of the proposed scheme with different iterations and different encoders in suburban environment: (a) encoder (2,1,3) and (b) encoder (2,1,5).

Fourier transform (FFT) with size $M = 32$ and $N = 256$, so the load of system users can be up to 8. In the CHATUE algorithm, a data frame is encoded by a convolution code. The code rate of the turbo code employed in the simulations is 1/2. The length of information bits in TEQ-CP is the same as that in CHATUE. We compared the TEQ performances with those of TEQ-CP, CHATUE1, and those of CHATUE2 with that of CHATES for the MU-MIMO SC-FDMA system. Here, we present the simulation results to verify the channel estimation accuracy improvement achieved by the proposed joint IBI cancellation and channel estimation technique, CHATES. Figure 2 shows the BER performances obtained with different iterations in the proposed system with different turbo encoders in a suburban channel environment. We can see that the performance with the fourth iteration is almost the same as that with the fifth iteration, so our proposed receiver converges at the fifth iteration. Without the IBI cancellation technique, the estimation accuracy degrades owing to IBI even after six iterations are performed. Figure 3 shows the BER performances obtained with different iterations and a different turbo encoder in an urban channel environment. Next, we present the BER performance of CHATUE2, and compare it with that of CHATUE1 and TEQ-CP. Figure 4 shows the BER performance comparisons of TEQ-CP, CHATUE1, and CHATUE2 with the CHATES algorithm under the conditions of six iterations and different channel environments for an MU-MIMO SC-FDMA system. We see that our proposed scheme outperforms the others. The

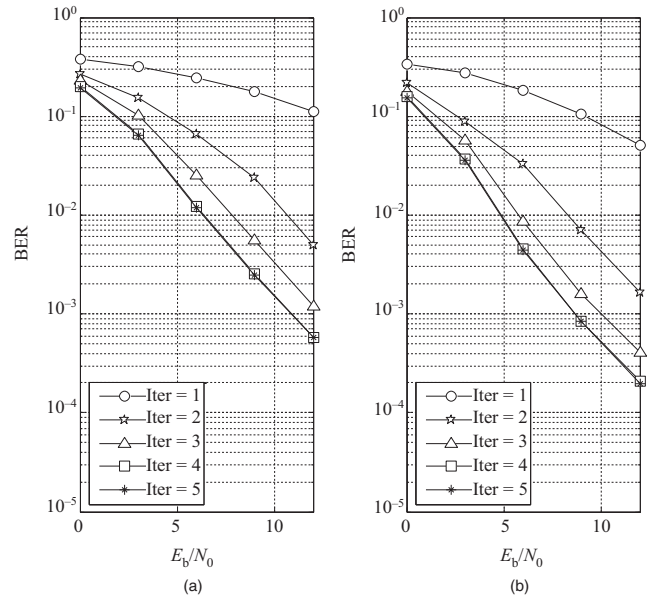


Fig. 3. Comparison of BER performance of the proposed scheme with different iterations and different encoders in an urban environment: (a) encoder (2,1,3) and (b) encoder (2,1,5).

proposed scheme has a better channel estimation property, and has a better BER performance than that of CHATUE1 because the proposed technique has a composite replica, which improves the SNR at the equalizer output. The proposed scheme with ideal channel estimation outperforms the existing scheme TEQ-CP. Figure 5 shows the BER performances of TEQ-CP, CHATUE2 with the CHATES algorithm, and CHATUE2 with known channel information

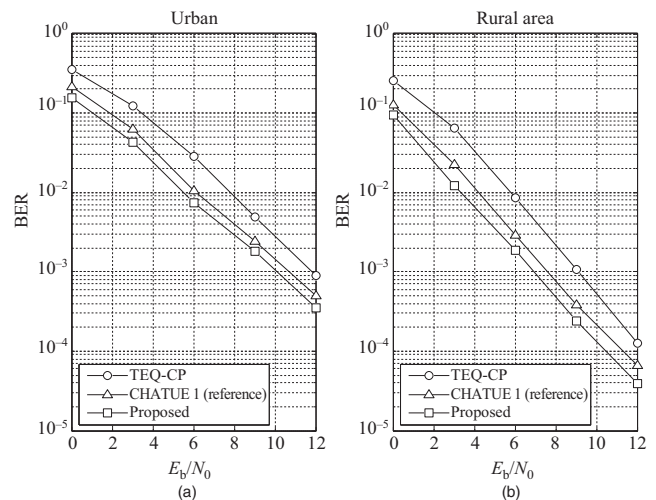


Fig. 4. Comparison of BER performance of the proposed scheme with existing schemes (TEQ-CP and CHATUE1) and with six iterations: (a) urban environment and (b) rural environment.

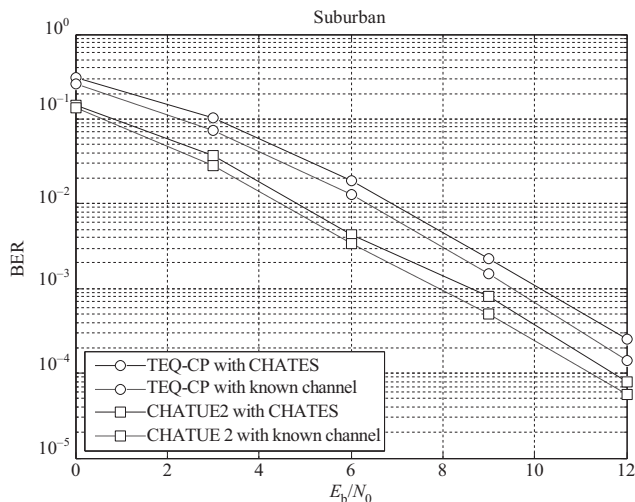


Fig. 5. Comparison of BER performance of the proposed scheme and existing TEQ-CP (with CHATES and known channel).

in a suburban environment. We see that the channel estimation of CHATES approaches that of the true channel.

V. Conclusion

The proposed scheme is shown to have good spectrum efficiency and achieves good channel estimation. Compared with the existing methods, the proposed scheme meets the requirements for practical implementation. It is preferable to minimize the length of the CP to improve the transmission energy and spectrum efficiency. The use of CHATUE with CHATES is employed in the designed receiver. CHATES employs a short TR and can improve the spectrum efficiency without sacrificing the estimation accuracy. Some simulation examples are given to demonstrate the effectiveness of the proposed scheme.

References

- [1] H.G. Myung, J. Lim, and D.J. Goodman, "Single Carrier FDMA for Uplink Wireless Transmission," *IEEE Veh. Technol. Mag.*, vol. 1, no. 3, Sept. 2006, pp. 30–38.
- [2] H. Li and H. Liu, "An Analysis on Uplink OFDMA Optimality," *IEEE Trans. Wireless Commun.*, vol. 6, no. 8, Aug. 2007, pp. 2972–2983.
- [3] C. Ciochina, D. Castelain, D. Mottier, and H. Sari, "Space-Frequency Block Code for Single-Carrier FDMA," *IEEE Electron. Lett.*, vol. 44, no. 11, 2008, pp. 690–691.
- [4] H. Jafarkhani, *Space-Time Coding: Theory and Practice*, Cambridge, UK: Cambridge University Press, 2005.
- [5] C.-W. Tan and A.R. Calderbank, "Multiuser Detection of Alamouti Signals," *IEEE Trans. Commun.*, vol. 57, no. 7, 2009, pp. 2080–2089.
- [6] H.V. Poor, "Iterative Multiuser Detection," *IEEE Signal Proc. Mag.*, vol. 21, Jan. 2004, pp. 81–88.
- [7] S. Ahmed and S. Kim, "Efficient List-Sphere Detection Scheme for Joint Iterative Multiple-Input Multiple-Output Detection," *IET Commun.*, vol. 8, no. 18, Dec. 2014, pp. 3341–3348.
- [8] C. Zhang and Z. Wang, "Frequency Domain Decision Feedback Equalization for Uplink SC-FDMA," *IEEE Trans. Broadcast.*, vol. 56, no. 2, Apr. 2010, pp. 253–257.
- [9] G. Huang, A. Nix, and S. Armour, "Decision Feedback Equalization in SC-FDMA," in *Proc. Int. Symp. IEEE PIMRC*, Cannes, France, Sept. 15–18, 2008, pp. 1–5.
- [10] Y. Takano, K. Anwar, and T. Matsumoto, "Spectrally Efficient Frame-Format-Aided Turbo Equalization with Channel Estimation," *IEEE Trans. Veh. Technol.*, vol. 62, no. 4, 2013, pp. 1635–1645.
- [11] K. Anwar and T. Matsumoto, "Low Complexity Time-Concatenated Turbo Equalization for Block Transmission without Guard Interval: Part 1 - The Concept," *Springer Wireless Pers. Commun.*, vol. 67, no. 4, Mar. 2012, pp. 761–781.
- [12] D. Wang, C. Wei, Z. Pan, X. You, C.H. Kyu, and J.B. Jang, "Low-Complexity Turbo Equalization for Single-Carrier Systems Without Cyclic Prefix," in *Proc. IEEE Int. Conf. Commun. Syst.*, Guangzhou, China, Nov. 19–21, 2008, pp. 1091–1095.
- [13] M. Nicoli, S. Ferrara, and U. Spagnolini, "Soft-Iterative Channel Estimation: Methods and Performance Analysis," *IEEE Trans. Signal Process.*, vol. 55, no. 6, June 2007, pp. 2993–3006.
- [14] K. Kansanen, "Wireless Broadband Single-Carrier Systems with MMSE Turbo Equalization Receivers," Ph.D. dissertation, Dept. Electr. Inform. Eng., Univ. Oulu, Finland, 2005.
- [15] H. Zhou, K. Anwar, and T. Matsumoto, "Chained Turbo Equalization for SC-FDMA Systems Without Cyclic Prefix," in *Proc. IEEE Globecom Workshops*, Miami, FL, USA, Dec. 6–10, 2010, pp. 1318–1322.
- [16] Z. Chen, Y. Chang, F. Liu, J. Zhou, and D. Yang, "A Turbo FDE Technique for OFDM System Without Cyclic Prefix," in *Proc. IEEE VTC*, Anchorage, AK, USA, Sept. 22–23, 2009, pp. 1–5.
- [17] H. Lee, Y. Lee, K. Ahn, and H. Park, "Interference Cancellation for Single Carrier Frequency Domain Equalizer without Cyclic Prefix," in *Proc. IEEE VTC*, Taipei, Taiwan, May 16–19, 2010, pp. 1–4.
- [18] B. Sah, M. Surendar, and P. Muthuchidambaramanathan, "A Frequency Domain Joint MMSE-SIC Equalizer for MIMO SC-FDMA LTE-A Uplink," in *Proc. IEEE Conf. Electron. Commun. Syst.*, Coimbatore, India, Feb. 13–14, 2014, pp. 1–4.

- [19] H.-M. Kim, D. Kim, T.-K. Kim, and G.-H. Im, "Frequency Domain Channel Estimation for MIMO SC-FDMA Systems with CDM Pilots," *IEEE Commun. Netw.*, vol. 16, no. 4, Aug. 2014, pp. 447–457.
- [20] A. Kiayani, L. Anttila, Y. Zou, and M. Valkama, "Channel Estimation and Equalization in Multi-User Uplink OFDMA and SC-FDMA Systems Under Transmitter RF Impairments," *IEEE Trans. Veh. Technol.*, vol. 65, no. 1, Jan. 2016, pp. 82–99.
- [21] I.A. Xirouchakis, "Spatial Channel Model for Multiple Input Multiple Output (MIMO) Simulations A Ray Tracing Simulator Based on 3GPP TR 25.996 v. 6.1.0," Physics Department, University of Athens, July 31, 2008.



Hung-Sheng Wang was born in Taipei, Taiwan, on July 1991. He received the B.S. degree from the Department of Aeronautical Engineering, National Formosa University, Yunlin, Taiwan, in 2013, and the M.S. degree in communication engineering from the National Chung Hsing University (NCHU), Taichung, Taiwan, in 2015. He was a member of the Electronic Communication Systems Laboratory at NCHU. His research interests include Long-Term Evolution (LTE), multiple antenna communications, turbo equalization, and channel estimation.



Fang-Biau Ueng received the Ph.D. degree in electronic engineering from the National Chiao Tung University, Hsinchu, Taiwan in 1995. From 1996 to 2001, he was with the National Space Program Office of Taiwan as an associate researcher. From 2001 to 2002, he was with Siemens Telecommunication Systems Limited, Taipei, Taiwan, where he was involved in the design of mobile communication systems. Since February 2002, he has been with the Department of Electrical Engineering, National Chung-Hsing University, Taichung, Taiwan. His areas of research interest are wireless communication and adaptive signal processing.



Yu-Kuan Chang was born in Kaohsiung, Taiwan, in 1986. He received the B.Sc. degree in aeronautical engineering from National Formosa University, Yunlin, Taiwan, in 2008, and the M.Sc. degree from the National Chi Nan University, Nantou, Taiwan, in 2010. He is a member of the Communications System Laboratory, National Chung Hsing University. His research interests are MIMO MC-CDMA and LTE communication systems.